PHYSICAL REVIEW B **67**, 035118 (2003)

Magneto-optical Kerr effect in Pr monopnictides

Dipta Bhanu Ghosh, Molly De, and S. K. De
Department of Materials Science, Indian Association for the Cultivation of Science, Jadavpur, Kolkata 700 032, India

(Received 16 May 2002; revised manuscript received 13 September 2002; published 30 January 2003)

The electronic and magneto-optical properties of Pr monopnictides have been studied from the self-consistent electronic structure calculation employing full potential linear muffin-tin orbital method. The local spin density approximation along with on site Coulomb interaction (LDA+U) is used for electronic structure calculation. The inclusion of U in LDA results in low density of states at the Fermi level which imply that Pr monopnictides are semimetals. The spin and orbital magnetic moments primarily arise from the *f* states. The Kerr spectra are significant with sharp and large rotation of $-5°$ at the lower energy region. The occupied *f* states are approximately 4 eV below Fermi level and do not contribute directly to optical transitions in the interested range of energy. These investigations suggest that the plasma frequency and the orbital magnetic moment play key roles for determining the magneto-optical spectra.

DOI: 10.1103/PhysRevB.67.035118 PACS number(s): 78.20.Ls, 71.28.+d

I. INTRODUCTION

The discovery of giant Kerr rotation of about 90° in CeSb created a renewed interest in the magnetic and the magneto-optical properties of rare-earth (RE) compounds.[1] Before this discovery, very few novel materials showing magneto-optical Kerr effect (MOKE) were known. Among these were Fe, Co, and Ni, where the polar Kerr rotation is typically in the range of 0.3° to 0.6° for optical frequencies. In order to obtain large rotations, the obvious choice will be a material with large spin-orbit (SO) coupling, large magnetic moments, and particular optical resonances in only one spin type. MOKE has been observed in compounds containing light rare-earth ions such as Ce^{+3} and Nd^{+3}, Eu^{+2} with half-filled $4f$ shell and heavy RE such as Tm^{+3} and Yb^{+3} and in uranium chalcogenides.[2] Polar Kerr rotation in UX (X=S, Se, Te) is one order of magnitude larger than that of Fe, Co, and Ni.[3] However, some light RE compounds exhibit a rotation of magnitude much higher compared to the transition elements and U chalcogenides. Previous experiment[4] on CeSb produced a large rotation of 14° at 0.55 eV. Pittini *et al.*[1] recorded highest 90° rotation at about 0.4 eV in addition to that at 0.55 eV. Such an unusual Kerr rotation observed in CeSb demands a new model for describing the *f* electrons and their interaction with the *d* electrons of Ce and *p* electrons of Sb.

In order to gain an insight into the unusually high Kerr rotation in CeSb and moderately large ones in CeS, NdS, and CeTe, various computational schemes have been suggested. The density functional theory (DFT) in the local spin density approximation (LSDA) explains the MO Kerr spectra of transition-metal compounds[5,6] and alloys satisfactorily in most cases. However, it fails totally in case of $4f$ and Mott-Hubbard Insulator compounds.[7,8] The singular theoretical[9] work on PrSb treated the $4f$ states as core ones and used the crystal field approach to calculate the magnetic moment and Kerr rotation in presence of external magnetic field. In spite of the magnetic moment being correctly reproduced, both the Kerr rotation and reflectivity spectra agree very poorly with the experimental results. It follows that both LSDA and treating $4f$ as core states are insufficient in obtaining the appropriate electronic structure of light rare-earth compounds. Various modifications such as self-interaction-corrected calculations,[10] LDA+U and combination of LDA calculated parameters with model Hamiltonians have been used in RE compounds[11]. The LDA+U method leads to a MOKE spectra which show best matching with experimental results in case of RE compounds. Theoretical investigations using this method have been performed on CeSb (Refs. 12,13) and Ce, Nd, and Tm monochalcogenides.[13–15] MOKE spectra obtained tallies fairly well with the experiment and the magnetic moments calculated are close enough to the measured ones. In case of Nd and Tm monochalcogenides, the futility of treating the $4f$ electrons as core electrons have been studied. LDA+U calculations on YbBiPt reproduces its heavy-fermion[16] nature. Till now, the strongly correlated systems are not fully understood. Furthermore the orbital moment in *f* systems is not quenched and the orbital dependency of the potential describing the *f* electrons is most essential. This is also achieved in LDA+U method. Among all these RE compounds, the Pr monpnictides are not investigated in details. Though the *f* electrons, such as those in CeSb, are not fully localized, PrSb (Ref. 17) does not exhibit giant Kerr rotation. In spite of being a light rare-earth compound, PrSb produces a Kerr signal of only 0.4°. The magnetic moment is also small, about $0.9\mu_B$/f.u. at 4.2 K, unusual for a RE compound. CeS, inspite of its small magnetic moment[18] exhibits giant Kerr signal. The inadequacy in the treatment of the $4f$ electrons in the only published work[9] on PrSb demands a further thorough investigation of PrSb, taking into account the strong correlation among the $4f$ electrons. It was our endeavor to investigate whether the LDA+U scheme describes the electronic structure, magnetic, and magneto-optical properties as accurately in Pr monopnictides as in Ce monopnictides and also as to why PrSb exhibits such a small rotation.

II. CALCULATIONAL DETAILS

Full potential (FP) self-consistent spin-polarized band structure calculations have been performed on Pr monopnictides PrX (X=P, As, Sb, Bi) by the linear muffin-tin orbital method (LMTO)[19] using the FP-LMTO code developed by Savrasov *et al.*[20] The DFT is modified in order to include the strong correlations among the f electrons. In the LDA+U method,[11] the LDA energy functional is modified by removing the LDA f-f interactions and adding the strong on-site Coulomb interactions among the f electrons. The main idea of the LDA+U method used in this calculation is that the LDA gives a good approximation for the average Coulomb energy of f-f interactions E_{av} as a function of the total number of f electrons $N=\Sigma_{m\sigma}n_{m\sigma}$, where $n_{m\sigma}$ is the occupancy of a particular $f_{m\sigma}$ orbital

$$E_{\mathrm{av}}=U\frac{N(N-1)}{2}-J\frac{N(N-2)}{4}. \tag{1}$$

Subtracting E_{av} from the LDA total-energy functional, and adding orbital- and spin-dependent contributions to obtain the exact (in the mean-field approximation) formula for total energy, i.e.,

$$\begin{aligned} E=E_{\mathrm{LDA}}-\left(U\frac{N(N-1)}{2}-J\frac{N(N-2)}{4}\right) \\ +\frac{1}{2}\sum_{m,m',\sigma}U_{mm'}n_{m\sigma}n_{m'-\sigma} \\ +\frac{1}{2}\sum_{m\neq m',m',\sigma}(U_{mm'}-J_{mm'})n_{m\sigma}n_{m'\sigma}. \end{aligned} \tag{2}$$

The derivative of above equation with respect to orbital occupancy $n_{m\sigma}$ gives the expression for the occupation-dependent one-electron potential

$$V_{m\sigma}(\mathbf{r})=\frac{\delta E}{\delta n_{m\sigma}} \tag{3}$$

or

$$\begin{aligned} V_{m\sigma}(\mathbf{r})=V_{\mathrm{LDA}}(\mathbf{r})+\sum_{m'}U_{mm'}n_{m'-\sigma}+\sum_{m'\neq m}(U_{mm'} \\ -J_{mm'})n_{m\sigma}-U\left(N-\frac{1}{2}\right)+J\left(n_{\sigma}-\frac{1}{2}\right), \end{aligned} \tag{4}$$

where $n_{\sigma}=Tr(n_{mm',\sigma})$. The Coulomb and exchange matrices $U_{mm'}$ and $J_{mm'}$ are

$$U_{mm'}=\sum_{k}a_kF^k, \tag{5}$$

$$J_{mm'}=\sum_{k}b_kF^k, \tag{6}$$

$$a_k=\frac{4\pi}{2k+1}\sum_{q=-k}^{k}\langle lm|Y_{kq}|lm\rangle\langle m'|Y_{kq}^{*}|lm'\rangle, \tag{7}$$

$$b_k=\frac{4\pi}{2k+1}\sum_{q=-k}^{k}|\langle lm|Y_{kq}|lm'\rangle|^2, \tag{8}$$

where $F^{k'}$s are Slater integrals and $0\leqslant k\leqslant 2l$. The Coulomb and exchange parameters are evaluated as

$$U=\frac{1}{(2l+1)^2}\sum_{mm'}U_{mm'}, \tag{9}$$

$$J=U+\frac{1}{2l(2l+1)}\sum_{mm'}(U_{mm'}-J_{mm'}). \tag{10}$$

TABLE I. The lattice parameter a, muffin-tin radii of Pr S_{Pr}, and pnictogen S_X, Fermi level E_F, density of states at Fermi level $N(E_F)$, plasma frequency ω_{pl} and DOS due to f electrons at E_F,f_{DOS}.

	a (a.u.)	S_{Pr} (a.u.)	S_X (a.u.)	E_F (eV)	$N(E_F)$ (St./eV)	ω_{pl} (eV)	f_{DOS} (St./eV)
PrP	11.159	3.013	2.567	8.278	0.144	1.395	0.017
PrAs	11.395	3.019	2.678	8.262	0.165	1.422	0.023
PrSb	12.046	3.071	2.951	7.942	0.394	1.584	0.126
PrBi	12.210	3.113	2.991	8.169	2.249	1.772	1.734

The value of $F^0(=U)$ is chosen to be 6.5 eV since its value for rare-earth compounds lies in the range 5–7 eV. The other Slater integrals F^2, F^4, and F^6 for f electrons have been used from the experimental paper by Thole *et al.*[21] to calculate the matrices $U_{mm'}$ and $J_{mm'}$. The exchange-correlation potential in the LDA was calculated with Vosko-Wilk-Nussair parametrization. The experimental[22] lattice parameters for PrP, PrAs, PrSb, and PrBi are given in Table I. They have rock-salt type structure at ambient conditions. The basis consists of Pr: $6s$, $5p$, $5d$, $4f$ and pnictogen: $(n)s$, $(n)p$ and $(n)d$, where n refers to the principal quantum number. The $5s$ electrons of Pr and $(n-1)d$ electrons of Sb and Bi were treated in a separate panel and hence were not included in the optical calculations. Charge density, density of states and the momentum matrix elements were calculated on a grid of 242 **k** points in irreducible Brillouin zone and the **k** space integration was performed using the tetrahedron method. We have treated orbital momentum quantum number, m_l as a parameter and tried several combinations to obtain as close result as obtained in experiment.[17] LSDA calculation on PrSb has also been performed. Furthermore, in order to bring about the effect of U on the band structure and the Kerr rotation, more calculations with $U=5.5$ eV and $U=7.0$ eV have been carried out on PrSb with the same m_l combination.

III. RESULTS AND DISCUSSION

The energy band structure of Pr monopnictides calculated is substantially different from the traditional LDA or LSDA calculation, performed previously.[23,25] Figure 1 shows the energy band structure of PrSb. We have laid special emphasis on PrSb since the experimental data is available for PrSb only. The lower Hubbard f bands of Pr occur at about 4 eV below the Fermi level (E_F). The two Pr f bands are about 0.5 eV apart and are almost dispersionless. The phosphorus p

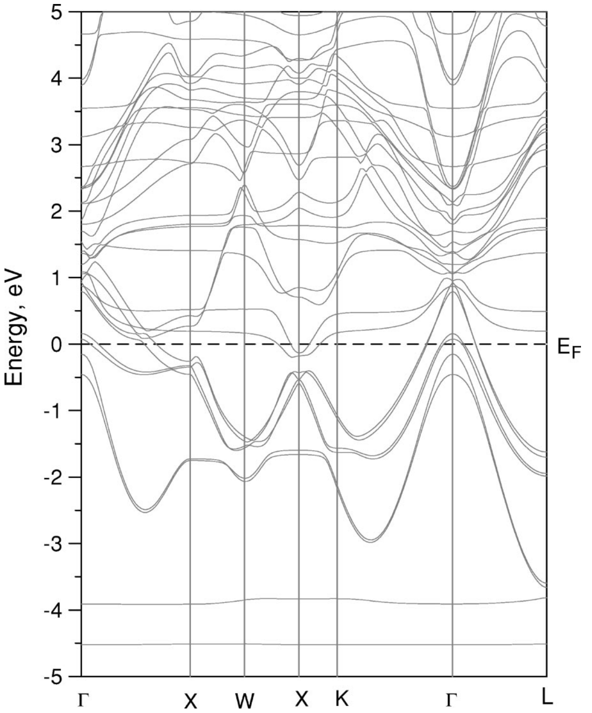

FIG. 1. Band structure of PrSb.

and Pr d hybridized bands are located in the vicinity of E_F. The conduction band consists of the unoccupied upper Hubbard f bands hybridized with Pr d bands.

Table I also provides information on E_F, density of states at E_F and the bare plasma frequency. Figure 2 shows the density of states of PrX (X=P, As, Sb, Bi). It is clear from the figure that there is a small amount of p-f hybridization at the bottom of the p band in the valence band. Such hybridization is also observed in Ce and Nd monopnictides,[14] albeit to a greater extent. Pnictogen p and Pr d hybridized bands are situated below E_F. Due to the increasing spin-orbit energy, given in Table II, as pnictogen is changed from phosphorus to bismuth, these bands show increasing splitting and widening. Apart from the splitting of the p-d hybridized bands below E_F and the shifting of the f-d hybridized bands towards E_F, there is qualitative similarity in the electronic structure of the Pr monopnictides. In PrBi, the Pr f state appears just below E_F. The small density of states at E_F of all the PrX suggest that they are all low-density carrier semimetals except PrBi. Information on the spin and orbital moment due to each atom and total magnetic moment in all the Pr monopnictides are given in Table II. Total magnetic moment is about $-3\mu_B$ in PrSb, which is considerably higher than the experimental magnetic moment[17] of about $0.9\mu_B$/f.u.. The computed orbital moment[24] in CeSb is $2.86\mu_B$ whereas it is about $-4.9\mu_B$ in PrSb. Hence orbital polarization of the $4f$ orbitals in PrSb is qualitatively different from that in CeSb. The m_l characters of the occupied $4f$ orbitals are -3 and -2 in PrSb. In the other monopnictides, since experimental data is not available, the same m_l combination has been applied. There is a consistency in the orbital moment of the PrX since the same configuration has been used. Total magnetic moments in all the PrX are more or less similar and are close to $-3\mu_B$. The contribution of the spin-orbit interaction towards the orbital polarization is not large. However the spin-orbit energy is highest in PrBi followed by PrSb and then by PrAs and PrP.

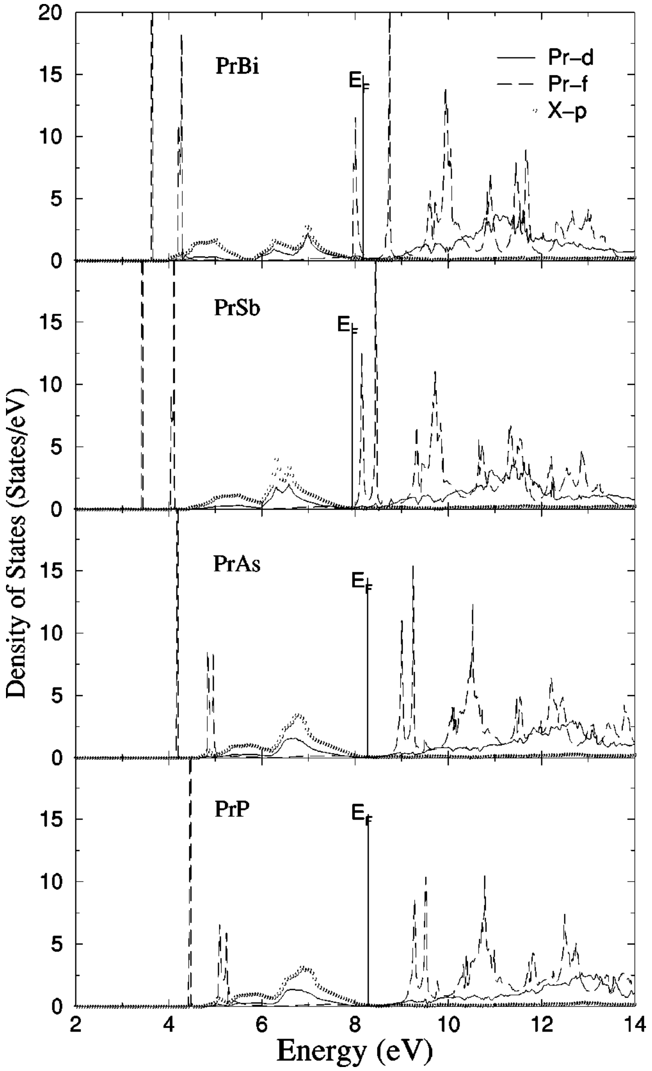

FIG. 2. l-projected density of states of Pr monopnictides.

Optical conductivity tensor has been calculated from the standard relations given by Reim *et al.*[2] The imaginary component of diagonal optical conductivity (σ^2_{xx}) and the real component of off-diagonal conductivity (σ^1_{xy}) have been calculated using the Kramers-Kronig transformation. Magneto-

TABLE II. Table contains E_{SO}, the spin-orbit energy, m_o and m_s, the atomic orbital and spin moments, respectively, and the total moment m_s+m_o.

	E_{SO} (meV)	m_s (Pr) μ_B	$m_s(X)$ μ_B	m_o (Pr) μ_B	$m_o(X)$ μ_B	m_s+m_o μ_B
PrP	124.75	1.89	−0.04	−4.86	0.00	−3.01
PrAs	128.34	1.89	−0.04	−4.87	0.00	−3.02
PrSb	141.93	1.96	−0.05	−4.91	0.01	−2.99
PrBi	361.28	2.06	−0.04	−4.93	0.00	−2.91

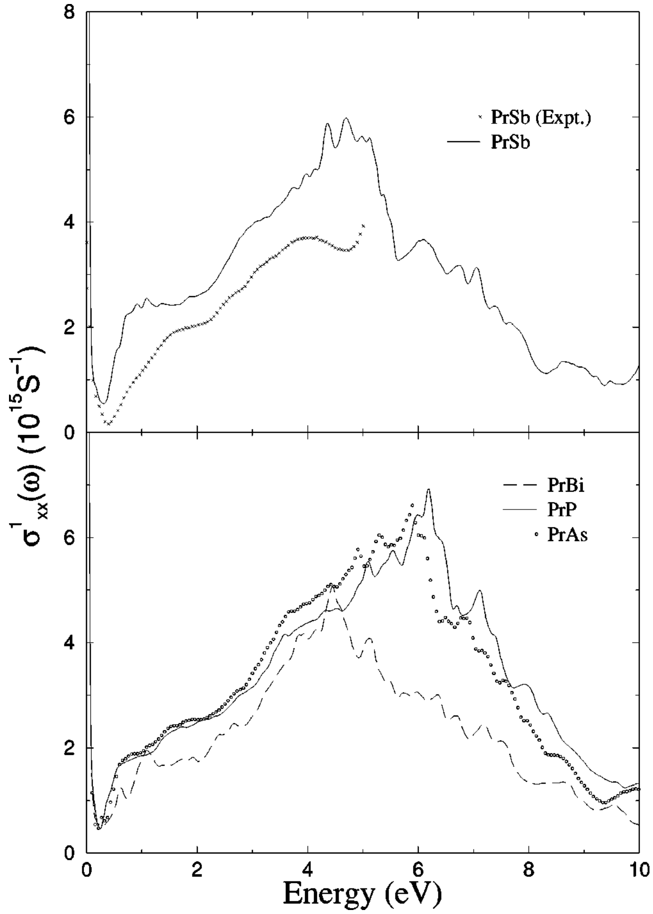

FIG. 3. Calculated absorptive component of diagonal optical conductivity of Pr monopnictides and the corresponding experimental (Ref. 17) spectrum for PrSb.

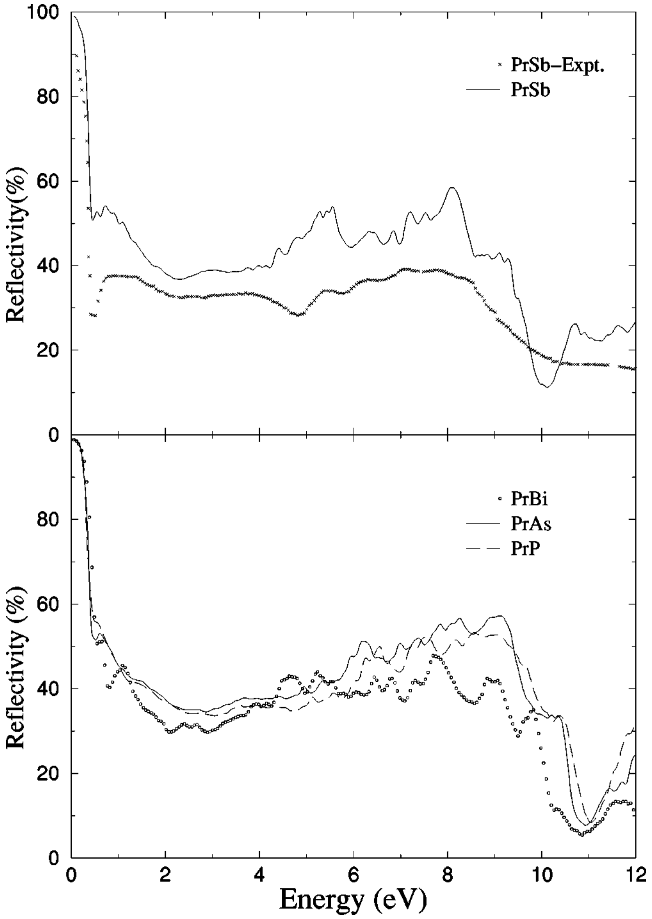

FIG. 4. Calculated reflectivity spectra of Pr monopnictides and the experimental (Ref. 17) reflectivity spectrum of PrSb.

optical Kerr rotation is calculated from the relation

$$\Phi_k = \theta_k(\omega) + i\epsilon_k(\omega) \approx \frac{-\sigma_{xy}}{\sigma_{xx}\sqrt{1+\frac{4\pi i}{\omega}\sigma_{xx}}}, \tag{11}$$

where σ_{xx} and σ_{xy} are the diagonal and off-diagonal components of the optical conductivity tensor, provided both are small and $|\sigma_{xy}| \ll |\sigma_{xx}|$. Here θ_k and ϵ_k are Kerr rotation and Kerr ellipticity, respectively.

Optical and magneto-optical spectra have been calculated for all the PrX using the LMTO band structure and further, a Lorentzian broadening of about 0.0136 eV has been used in order to obtain the best agreement with the experimental results of PrSb. Bare plasma frequency is also obtained from the LMTO band structure calculation. Hence only broadening has been used as a variable parameter. Figure 3 shows the calculated real part of the diagonal optical conductivity spectrum of PrX and the corresponding experimental spectrum for PrSb. A plasma minimum near 0.41 eV is shown in PrSb. Similar effect is seen in all the other PrX, with the plasma minima frequencies lying at 0.47, 0.43, and 0.5 eV in PrP, PrAs, and PrBi, respectively. The plasma frequency in CeSb was reported to be 0.4 eV and in case of NdS, NdSe, and NdTe were 2.91, 2.67, and 2.19 eV, respectively. The minima are obtained after applying Drude correction for intraband transitions. The only major peak occurs at 5 eV. This peak lies in a broad structure which is due to transitions from the p-d hybridized bands below and above E_F. There may be transitions from the dispersionless $4f$ bands in the valence band to the f-d hybridized band in the conduction band. But this takes place at higher energies. The structures above 10 eV are not considered by us since experimental data is not available in that range. In the other PrX, the spectra are qualitatively similar. The peak due to transitions from p-d hybridized bands $\rightarrow f$-d hybridized bands shifts to lower energies as we move to higher pnictides and the magnitude of the peak falls. This shifting to lower energies is obvious due to shifting of the f-d hybridized bands from higher energies towards E_F and the spin-orbit splitting of the p-d hybridized bands.

Calculated reflectivity spectra of PrX and the experimental one for PrSb are shown in Fig. 4. Not only PrSb but all the PrX exhibit plasma edge effect near 0.5 eV. The edge effect is considerably pronounced in PrSb and PrBi. There is considerable agreement with the experimental spectrum up to 10 eV. Optical conductivity calculations have been performed up to 40 eV for maximum accuracy in calculating $\sigma^2_{xx}(\omega)$ and $\sigma^1_{xy}(\omega)$. Figure 5 depicts

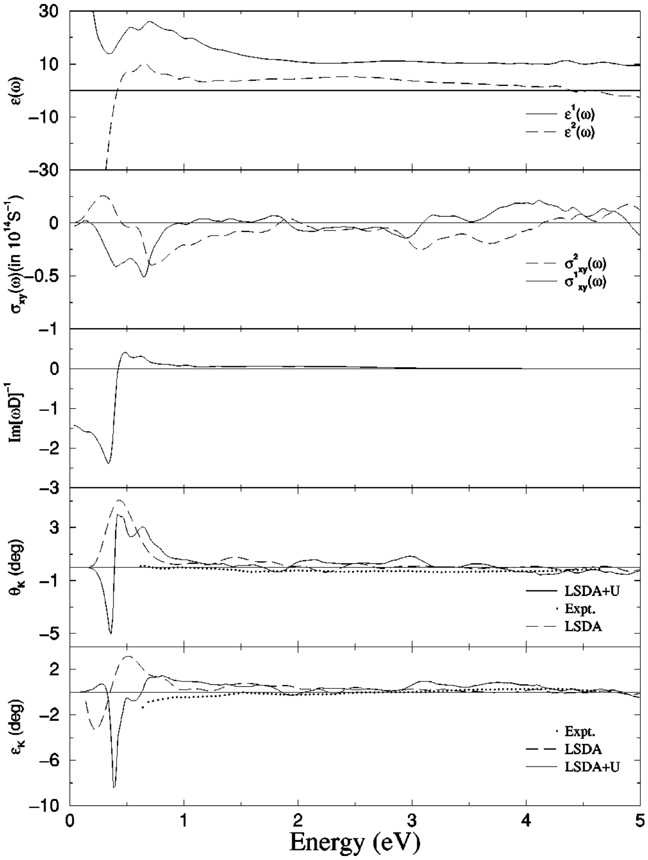

FIG. 5. Dielectric constant, off-diagonal conductivity Im $[\omega D]^{-1}$, Kerr spectra (calculated and experimental) of PrSb.

$\epsilon^1(\omega)$, $\epsilon^2(\omega)$, $\sigma^1_{xy}(\omega)$, $\sigma^2_{xy}(\omega)$, Im $[\omega D]^{-1}$ spectra, where $D=\sigma_{xx}\sqrt{1+(4\pi i/\omega)\sigma_{xx}}$, polar Kerr rotation and ellipticity of PrSb. The $\sigma^2_{xy}(\omega)$ spectrum shows a broad structures lying between 0.9 and 4 eV. Transitions involved in this range can be among the *p-d* hybridized bands. In this range, the calculated spectrum matches well with the experimental spectrum. However, the $\sigma^1_{xy}(\omega)$ spectrum shows a marked difference at low energy. The Im $[\omega D]^{-1}$ spectrum demonstrates the importance of the plasma edge since the only major peak occurs at an energy where the plasma edge is observed.

Kerr rotation is a manifestation of many phenomena. Spin-polarization, spin-orbit interaction, plasma minima or edge effect, joint density of states, momentum matrix elements, and orbital polarization all play important roles in determining the magneto-optical Kerr spectra. The polar Kerr rotation spectrum will follow the off-diagonal conductivity spectrum since the latter carries all the information regarding the spin polarization, spin-orbit interaction and the interaction between the two. However, plasma edge is also known to play a crucial role. Figure 6 shows the polar Kerr rotation and ellipticity spectra for PrP, PrAs and PrBi. Several structures of magnitudes varying between $-0.8°$ and 1.0° occur between 1 and 5 eV. Experimentally in PrSb, these structures are of about 0.4° and occur between 2 and 4 eV. For better understanding, the calculated θ_k and ellipticity spectra in the LDA+U scheme and in the LSDA scheme have been compared with the measured ones in Fig. 5. Here again, the ellipticity spectrum seems to follow the experimental spectrum. Hence, one can say that the complex Kerr rotation spectra are close enough. But LSDA results exhibit significant deviation from the experimental ellipticity spectrum. The sharpness of the peak seen in Nd and Tm monochalcogenides[14,15] at the plasma minima and plasma edge, respectively, is also observed in PrSb. The most interesting feature is that the largest peaks are found to be near 0.5 eV, in all the PrX. Since the plasma edge effect also occurs at the same energy, it is of crucial importance in magneto-optical Kerr rotation phenomenon. Among the Pr monopnictides, PrSb shows the highest Kerr rotation of about $-5°$. The other Pr monopnictides exhibit smaller rotations. One can safely rule out orbital magnetism as the cause since all the Pr monopnictides have the same orbital moment. The origin of the larger Kerr rotation in PrSb can be traced from the pronounced plasma edge effect in PrSb. CeS, having a magnetic moment of $0.5\mu_B$, shows a large Kerr rotation[18] of 22°. The one common phenomenon in all the above mentioned rare-earth compounds showing large Kerr rotations is plasma minimum or plasma edge effect.

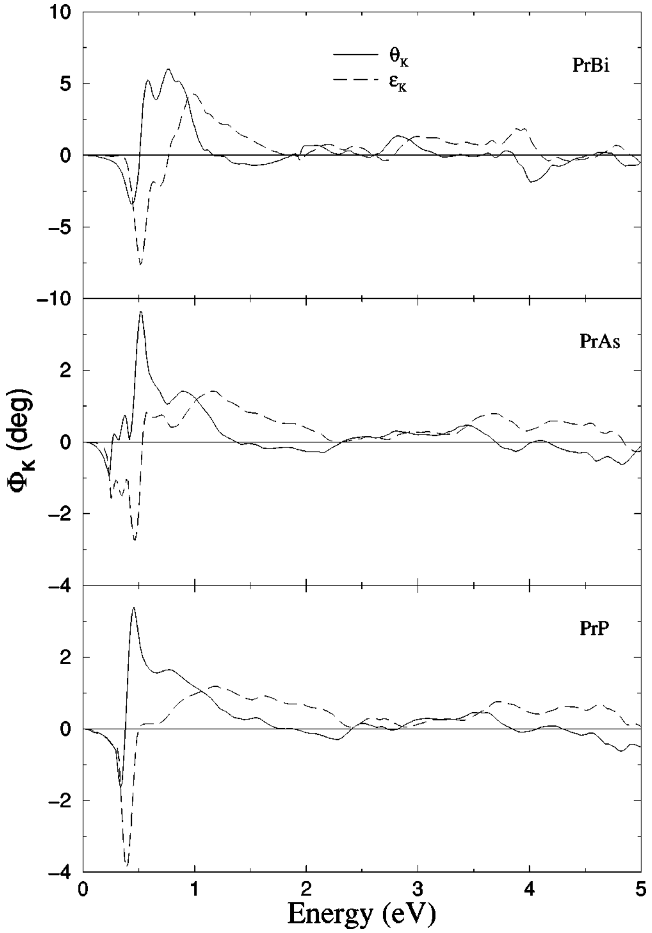

FIG. 6. Kerr rotation and ellipticity spectra of PrP, PrAs, and PrBi.

The off-diagonal conductivity spectra calculated in this paper is an improvement upon our previous work.[25] The LDA+U scheme chosen was that for the average occupancy and hence the m_l and spin configuration did not comply with Hund's rule. The calculation reported in this paper now involves a scheme given by Lichtenstein[26] and it improves our results. Although magnetic moment matching was not achieved, the Kerr rotation and reflectivity spectra are definitely an improvement over the previous work on PrSb.[9]

Since LDA+U method deals very superficially with the placing of the *f* electrons, it is essential to find out whether change in the value of U brings out any significant change in the band structure, p-f hybridization, and above all the MO properties of PrSb. Self-consistent calculations have also been carried out for $U=7.0$ and 5.5 eV. The band structure is negligibly affected if U is changed to 7.0 eV. However, there is a small change in the band structure when the Coulomb parameter is changed to 5.5 eV. The hitherto dispersionless occupied f bands move closer to the occupied p bands of antimony. The MOKE spectra remain virtually unaltered. Orbital moment remains close to $-4.9\mu_B$ in all the three cases. The diagonal conductivity spectra for the three different values of U remain almost similar. This obviously implies that the *f* electrons do not participate in the direct transitions but affect the MOKE spectrum through magnetic interactions. However, since the *f* states lie very close to the *p* states of Sb, it is essential to treat the *f* electrons as band states. But mere LSDA band treatment of the f electrons leads to wrong fermiology of the RE's. LDA+U leads to the correct fermi surface of PrSb. We have now compromised on the hybridization effects of f electrons with other orbitals. But since there is no major structure due to transitions from the *f* states, we can safely say that the LDA+U treatment of the Pr monopnictides do not lead to the wrong MOKE spectra. Since the Kerr rotation spectrum is not changed substantially if U is changed from 5.5 to 7.0 eV, one can say that LDA+U describes the electronic structure of the Pr monopnictides satisfactorily.

Although we have carried out calculations for various combinations of m_l, the best matching of both the orbital moment and the MOKE spectra of PrSb with the experiment is achieved for $m_l=-3$ and $m_l=-2$. In case of Nd monochalcogenides, best results[14] were reported for $m_l=0$ and $m_l=\pm 3$. However, best agreement[15] was achieved for $m_l=\pm 2$ in Tm monochalcogenides. This suggests that the chemical environment of Pr plays a significant role. Interestingly, the occupied $4f$ orbital in CeSb has $m_l=-3$ character,[12,24] yet in CeTe, $m_l=-2$ was the lowest occupied $4f$ state.[12] In the former, good agreement with MO spectrum was achieved but in case of the latter, both the magnetic moment and MO spectrum showed poor matching. Since the total magnetic moment in PrSb is an order higher than the experimental one, LDA+U is insufficient in reproducing the magnetic properties of PrSb. As there is no unique method of choosing the occupied $4f$ orbitals, this deficiency may be reflected in the magnetic moment.

IV. CONCLUSION

From the full potential band structure calculation for Pr monopnictides, one finds that LDA+U successfully calculates most features of the light rare-earth monopnictides, namely, low-carrier density semi-metals, f-d hybridization, orbital polarization. However van Vleck paramagnetism seen in PrSb is not reproduced. Obviously some other interaction is essential for obtaining the appropriate magnetic moment. The conductivity spectrum for PrSb is very similar to the experimental one. Polar Kerr rotation is more or less successfully calculated, inspite of the finding that the off-diagonal conductivity spectra do not exactly follow the experimental one at low energy. It is also found that the MOKE spectra remain similar in nature for PrSb as U value is increased from 5.5 to 7.0 eV. This suggests that LDA +U is essential for achieving the MOKE spectrum and it is indispensible for obtaining the correct fermiology of the Pr monopnictides. The maximum Kerr rotation occurs at plasma shoulder or edge and it is an essential factor in obtaining magneto-optical Kerr signals. The origin of magneto-optical Kerr effect is mainly an interplay of the orbital polarization, spin polarization, plasma resonance, and dipole transitions.

ACKNOWLEDGMENTS

This work is funded by the Department of Science and Technology, Government of India (Project No. SP/S2/M-50/98).

---

[1] R. Pittini, J. Schoenes, O. Vogt, and P. Wachter, Phys. Rev. Lett. **77**, 944 (1996).

[2] W. Reim and J. Schoenes, in *Ferromagnetic Materials*, edited by E. P. Wohlfarth and K. H. J. Buschow (North Holland, Amsterdam, 1990), Vol. 5, p. 133.

[3] P. M. Oppeneer, T. Maurer, J. Sticht, and J. Kubler, Phys. Rev. B **45**, 10 924 (1992).

[4] W. Reim, J. Schoenes, F. Hulliger, and O. Vogt, J. Magn. Magn. Mater. **54-57**, 1401 (1986).

[5] P. M. Oppeneer, V. N. Antonov, T. Kraft, H. Eschrig, A. N. Yaresko, and A. Y. Perlov, J. Appl. Phys. **80**, 1099 (1996).

[6] V. N. Antonov, P. M. Oppeneer, A. N. Yaresko, A. Y. Perlov, and T. Kraft, Phys. Rev. B **56**, 13 012 (1997).

[7] M. De and S. K. De, J. Phys.: Condens. Matter **11**, 6277 (1999).

[8] V. N. Antonov, B. N. Harmon, V. P. Antropov, A. Y. Perlov, and A. N. Yaresko, Phys. Rev. B **64**, 134410 (2001).

[9] P. Monachesi, Z. Domanski, and M. S. S. Brooks, Phys. Rev. B **50**, 1013 (1994).

[10] S. Svane, W. Timmerman, and Z. Szotek, Phys. Rev. B **59**, 7888 (1999).

[11] V. I. Anisimov, J. Zaanen, and O. K. Andersen, Phys. Rev. B **44**, 943 (1991); A. I. Lichtenstein, V. I. Anisimov, and J. Zaanen, *ibid.* **52**, R5467 (1995).

[12] D. L. Price, B. R. Cooper, S. P. Lim, and I. Avgin, Phys. Rev. B **61**, 9867 (2000).

[13] A. N. Yaresko, P. M. Oppeneer, A. Y. Perlov, V. N. Antonov, T. Kraft, and H. Eschrig, Europhys. Lett. **36**, 551 (1996).

[14] V. N. Antonov, B. N. Harmon, A. Y. Perlov, and A. N. Yaresko,

Phys. Rev. B **59**, 14 561 (1999).

[15] V. N. Antonov, B. N. Harmon, and A. N. Yaresko, Phys. Rev. B **63**, 205112 (2001).

[16] P. M. Oppeneer, V. N. Antonov, A. N. Yaresko, A. Y. Perlov, and H. Eschrig, Phys. Rev. Lett. **78**, 4079 (1997).

[17] J. Schoenes, H. Brandle, A. Weber, and F. Hulliger, Physica B **163**, 496 (1990).

[18] R. Pittini, J. Schoenes, and P. Wachter, Phys. Rev. B **55**, 7524 (1997).

[19] O. K. Andersen, Phys. Rev. B **12**, 3060 (1975).

[20] S. Y. Savrasov and D. Y. Savrasov, Phys. Rev. B **46**, 12 181 (1992); S. Y. Savrasov, *ibid.* **54**, 16 470 (1996).

[21] B. T. Thole, G. Van. der Laan, and J. C. Fuggle, Phys. Rev. B **32**, 5107 (1985).

[22] K. C. Turberfield, C. Passel, R. J. Birgeneau, and E. Buscher, J. Appl. Phys. **42**, 1753 (1971).

[23] M. De, P. K. Sinharoy, and S. K. De, Phys. Lett. A **249/1-2**, 147 (1998).

[24] A. I. Lichtenstein, V. P. Antropov, and B. N. Harmon, Phys. Rev. B **49**, 10 770 (1994).

[25] M. De and S. K. De, Physica B **281/282**, 453 (2000).

[26] V. I. Anisimov, F. Aryasetiawan, and A. I. Lichtenstein, J. Phys.: Condens. Matter **9**, 767 (1997).